Determining the Crystal Structure of Metal Alloys via X-ray Diffraction

Elisa Jacquet, An Vuong, Alev Orfi

McGill University Department of Physics

Supervisor: Prof. Brunner & Prof. Sankey

February 4, 2019

Abstract

X-ray diffraction can be used to obtain micro-structural quantities of metal alloys. The addition of two Voigt functions provides a good fit for the double peak structure of the x-ray diffraction profiles allowing the determination of the lattice parameters of cubic crystals. We analyzed copper nickel, copper gold, and lead tin alloys, determining their lattice parameters and making conclusions about their respective alloy structures. The lattice parameter of pure copper (Cu), nickel (Ni), lead (Pb) and tin (Sn) were found to be 3.626 ± 0.008 Å, 3.525 ± 0.001 Å, 4.953 ± 0.001 Å, and 6.462 ± 0.002 Å, respectively. Their literature counterparts are 3.6146Å, 3.5240Å, 4.9052 Å, and 6.4892 Å. It was determined that Vegard's law does not suffice in describing the relation between the lattice parameter of copper nickel alloys and the substance concentration. Both the ordered and disorded structures of copper gold (Cu_3Au) alloys were analyzed. In addition, it was determined that tin and lead stay isolated in a lead tin alloy.

Contents

1 Introduction

By definition, a crystal is a material that can be decomposed into a repeating pattern of a particular unit. This unit, called a crystal unit, is fully representative of the crystal as a whole, carrying in it all of the crystal's physical properties [1]. For this reason, the analysis of crystal structures gives properties of the crystal itself and thus essential to our understanding of different materials.

Crystals are characterized through the shape of their periodic structures. Each cell can be parameterized with three vectors, known as the crystallographic axes. Their lengths and angles are known as the lattice parameters of the unit cell [2]. All of the crystals analyzed in this report are cubic, allowing their size to be described with only one length, a. There are three Bravais lattice types which have cubic unit cells [3]. These further specify the structure of a cubic unit cell. These types are shown in figure 1.
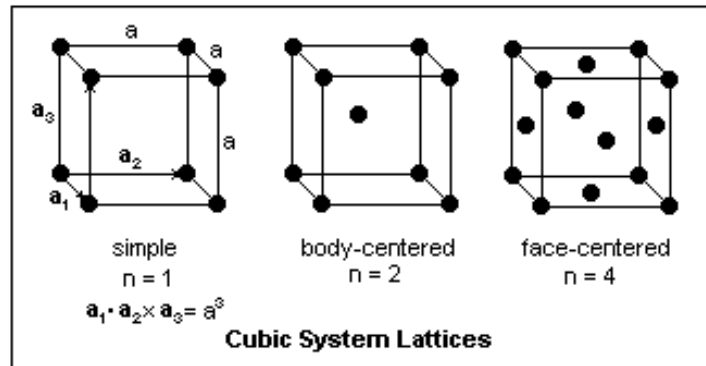

Figure 1: Different cubic structures. From left to right; simple cubic, body-centered cubic, and face-centered cubic [4].

The interaction of light with these crystals is dependent on the orientation of the planes. The direction of these planes can be symbolized using Miller indices which are defined as the reciprocal of the intercepts of the plane and the crystallographic axis. If h, k and l are the three Miller indices of a crystal with axial lengths a, b and c then the plane has intercepts a/h, b/k and c/l [3].

Crystal structures are generally studied through the diffraction of photons, neutrons and electrons. In this study, we use monochromatic x-rays and the rotating-crystal method to perform an analysis on the crystal structure of varying metal alloys. This method is dependent on Bragg's Law, a relation describing the creation of diffraction patterns when light interacts

with a crystal structure [3]. Consider two parallel planes separated by a distance d. The incident light reflects off both planes resulting in a path difference of the light. If this path different corresponds to an integral number of wavelengths there will be constructive interference. This occurs when the Bragg Law relation, shown below, is satisfied.

$$2d\sin\theta = n\lambda. \tag{1}$$

Here d is the distance between the planes, θ the incident angle of the x-ray, λ the wavelength of light and n any integer. This equation can be applied to crystal planes as well [3]. The relation between the inter-planar spacing d, the Miller indices and the lattice constants is dependent on the crystal system. The relation for the cubic system is shown below in equation 2 [3].

$$d = \frac{a}{\sqrt{h^2 + k^2 + l^2}}. \tag{2}$$

Recall a is the lattice parameter of a cubic cell, d the inter-planar spacing and h,k and l the Miller indices. Combining this relation and the Bragg Law we get a general relation for cubic structures.

$$\sin^2(\theta) = \frac{\lambda^2}{(4a^2)}(h^2 + k^2 + l^2). \tag{3}$$

The mathematical description of the amplitude and phase of a diffracted wave from a crystal lattice is known as the structure factor. This resultant wave is the summation of wave scattered by the individual atoms, given by the following equation [3].

$$F = \sum_n f_n \exp\left[-i2\pi(x_n h + y_n k + z_n l)\right]. \tag{4}$$

This sum is over all atoms in the unit cell. In equation 4 x_n, y_n, z_n are the positional coordinates of the nth atom, and f_n is known as the scattering factor of the nth atom. Using this equation we can find which Miller indices result in a peak in our diffraction pattern for different crystal structures. A body centered cubic structure has atoms at $x_1 = y_1 = z_1 = 0$ and $x_2 = y_2 = z_2 = \frac{1}{2}$ thus its structure factor is:

$$F = f_n[1 + \exp\left(-i\pi(h + k + l)\right)]. \tag{5}$$

This equation adds a restriction on the possible Miller indices create a peak as $F = 0$ if $h + k + l$ is odd, and $F = 2f$ if $h + k + l$ is even. This can be explained physically as a destructive interference of the diffracted light with those certain indices. Thus, when using equation 3 to find a we must only use even Miller indices.

For a face centered cubic, atoms have location $x_1 = y_1 = z_1 = 0, x_2 = 0, y_2 = z_2 = \frac{1}{2}, x_3 = z_3 = \frac{1}{2}, y_3 = 0, x_4 = y_4 = \frac{1}{2}, z_4 = 0$, thus a structure factor given by:

$$F = f[1 + \exp\left(-i\pi(k + l)\right) + \exp\left(-i\pi(h + l)\right) + \exp\left(-i\pi(h + k)\right). \tag{6}$$

This again restricts possible Miller indices, requiring them at all be odd or all be even. With these restrictions and knowledge of our sample crystal structure we can use equation 3 to obtain a value of the unit cell length a for each sample.

When preforming this same analysis on an alloy, the found value of a represents the average lattice parameter of the structure. Vegard's law states that this average lattice parameter often varies linearly with the alloy concentration [5]. A more detailed model, needed when Vegard's law doesn't hold, has additional non-linear terms. [6]. In our analysis we test this law with the copper nickel alloy.

Some alloys exhibit different crystal structures depending on the temperature at which they were formed [2]. For example copper gold alloys can exist in a disorder or ordered state. In the disorder state, the copper and gold atoms are arranged in random positions of a face centric cubic structure. In the ordered state the copper atoms occupy the face-centered positions and the gold atoms occupy the cube corner positions. This results in the ordered state behaving as simple cubic structure. These two states have practically the same lattice parameters but the difference in Bravais lattice structure results in additional reflections in the x-ray diffraction pattern of the ordered state [7].

2 Experimental Set-up

This study makes use of an x-ray diffractometer to obtain information about the crystal structure of various metal alloys. Such a diffractometer produces x-rays by decelerating and exciting electrons in a copper target. Through this process, an incident beam with two

wavelengths $k_{\alpha 1} = 0.15443$ nm and $k_{\alpha 2} = 0.15405$ nm is created. This beam is then incident on the sample at an angle θ. The sample diffracts the incident beam at varying angles depending on both θ and the sample's crystal structure, as explained in the introduction. A detector records the intensity of diffracted light at an angle 2θ. The sample and detector are rotated together so that the diffractometer can record at different incident angles (θ) ranging between 5°and 55°. A diagram of the basic set-up and geometry of the diffractometer is shown in figure 2.
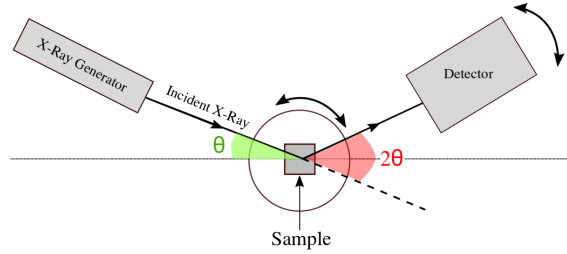

Figure 2: Diagram of the set-up of the x-ray diffractometer. The apparatus records the intensity of light at each angle 2θ.

The resulting data shows peaks at certain incident angles allowing the analysis of the samples crystal structure using equation 3. In our study, the experiment was conducted for alloys of copper and nickel, alloys of copper and gold, and alloys of lead and tin. For each sample, the apparatus counted the number of diffracted rays for 2 seconds, and rotated in intervals of 0.05°.

3 Analysis

3.1 Lattice Structure Determination

The diffraction patterns of three different sets of alloys were analyzed. These patterns consist of a number of peaks at values of 2θ, which vary by substance. A graphical representation of the raw data of the copper nickel alloys can be seen in figure 3, showing the changes in 2θ depending on concentration. The signal intensity tends to increase as the concentration of nickel in the studied alloy increases. Additionally, a slight right shift was also detected from all peaks as nickel's concentration dominates the alloy. A similar plot for copper gold can be found in appendix A.
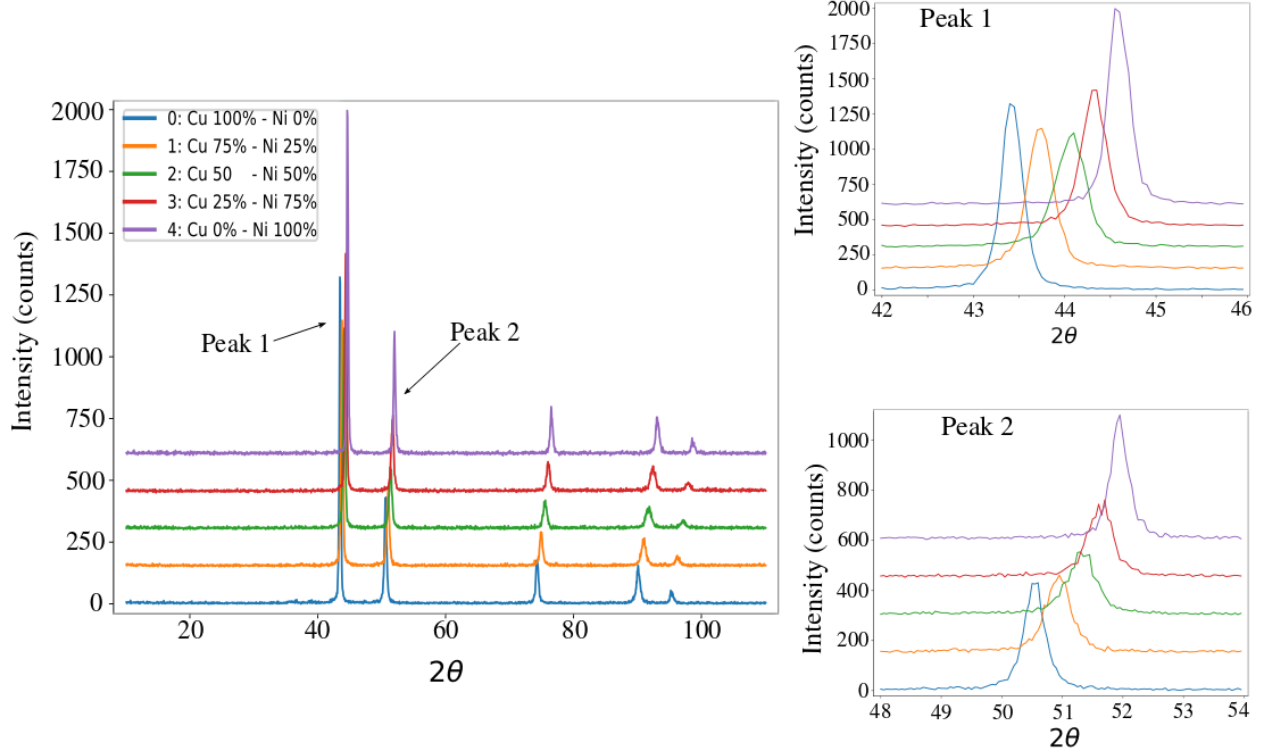
4

Figure 3: Plot of signal intensity verses angle 2θ of all five CuNi alloy samples with different concentration. LEFT: All data plotted on top of each other with a shift of 150 counts between 2 consecutive alloys. TOP RIGHT: Zoomed in image of peak 1. BOTTOM RIGHT: Zoomed in image of peak 2.

The different peaks in figure 3 correspond to the angles at which there is constructive interferes of diffracted x-ray. It is from these angles that the lattice constant, a, of the alloy can be extracted using equation 3. Copper, nickel, lead and gold all have face centered cubic centered structure thus restricting their miller indices to all be even or odd.

As mentioned previously, the x-ray incident upon the sample in the diffractometer is composed of the two k_α wavelengths of copper. For this reason, each apparent peak in figure 3 is a double peak. Each of these double peaks is modeled by the addition of two Voigt functions; where a Voigt function is a superposition of a Gaussian and Lorentzian curve. Each peak was individually fit to find an accurate value of 2θ for each wavelength. An example of this fit is shown in figure 4, where the peak fitting was performed on the second peak in the 100% Cu data series. The residuals plot of the same figure shows no systematic behavior. Furthermore, the success of the fit is confirmed by a reduced χ^2 value of 1.07 ± 0.17. A complete set of all 2θ values retrieved from the data for each alloy is tabulated in Appendix B. Only peaks with maximum intensity greater than 50 counts were

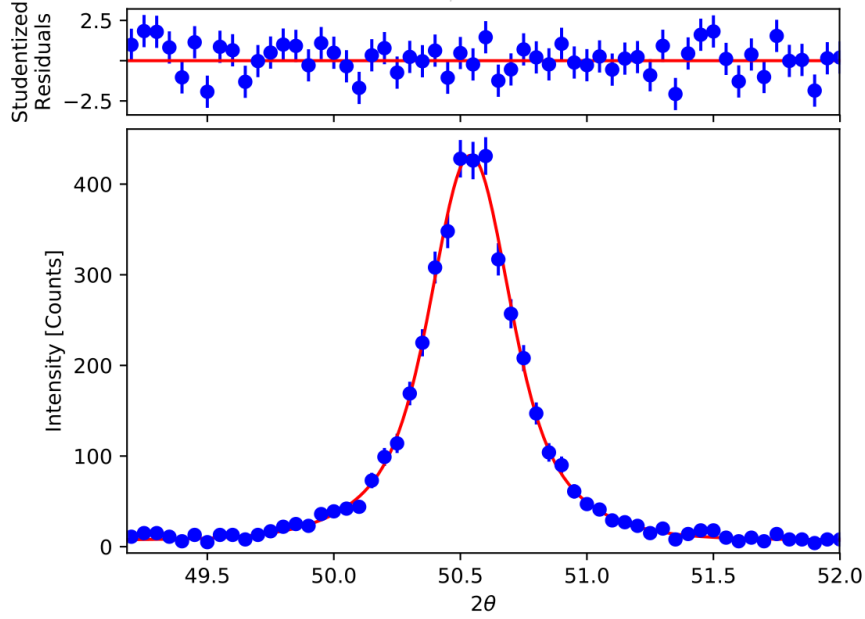considered distinct enough from background noise to be fitted.

Figure 4: Fitting on the 2nd double peak of Cu 100% alloy and its studentized residuals. Errors on the intensity were calculated by taking the square-root of the number of counts. Two Voigt functions with Gaussian standard deviation $\sigma_1 = 0.105 \pm 0.053$ and $\sigma_2 = 0.39 \pm 0.54$ and Lorentzian half-width $\Gamma_1 = 0.1 \pm 0.13$ and $\Gamma_2 = 0.2 \pm 1.5$ was used to fit this peak. Reduced chi-square value was calculated to be 1.07 ± 0.17 with 71 DOF. The peaks were identified to be at angles $2\theta_1 = 50.540 \pm 0.005°$ and $2\theta_2 = 50.53 \pm 0.02°$.

3.2 Crystal Structure of Copper Nickel

Copper nickel alloys of different concentration were analyzed using the double peak fitting outline above. We averaged the value of 2θ for each peak to get an average value for each double peak. Using a calculated value of 0.15424 nm for the average wavelength, a linear fit was preformed to determine the lattice constant,a, of each alloy. A sample plot of this fit is illustrated in figure 5. The coefficient of this linear fit was then used to calculate the lattice constant by the relation:

$$a = \frac{\lambda}{2 \times Slope}. \tag{7}$$

Lattice constants for the alloys are 3.626 ± 0.008 Å for 100% copper, 3.581 ± 0.004 Å for 75% copper and 25% nickel, 3.573 ± 0.004 Å for 50% copper and 50% nickel, 3.538 ± 0.009 Å for 25% copper and 75% nickel, and 3.525 ± 0.001 Å for 100% nickel. The literature values
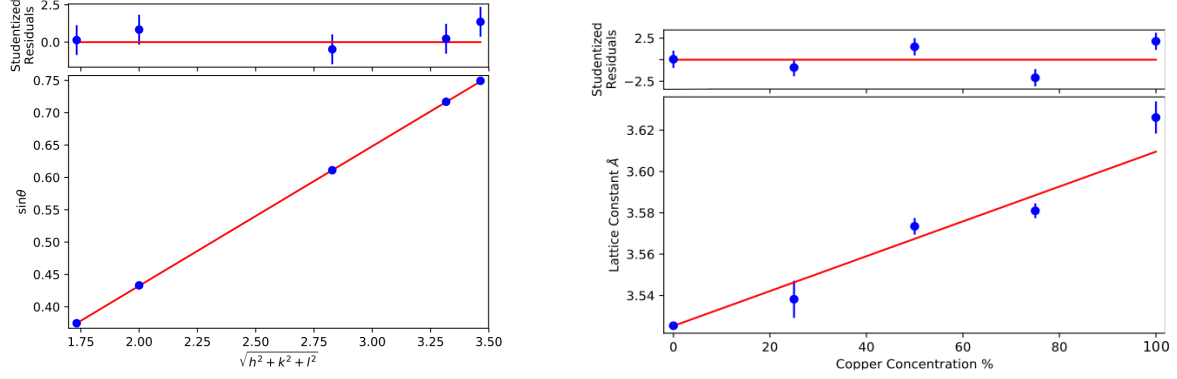
Figure 5: LEFT: A linear fit of the squared root sum of the 3 Miller indices squared versus $\sin\theta$ of Cu 50% Ni 50% alloy. The slope of this fit was determined to be 0.2158 ± 0.0002 with the y-intercept 0.0007 ± 0.0006. The reduced chi-square value is 0.95 ± 0.82. The lattice constant was determined to be 3.573 ± 0.004 Å. RIGHT: The plot of lattice constant versus copper concentration. The slope is $(8.4 \pm 0.2) \times 10^{-14}$ and y-intercept $(3.525 \pm 0.001) \times 10^{-10}$. The value of reduced chi-square is 3.99 ± 0.02.

are 3.6146 Å for copper and 3.5240 Å for nickel [5], showing the success of our process. A special note should be made that this results base on the assumption that there is no error on the wavelength.

Vegard's law, stating that the average lattice parameter varies linearly with the alloy concentration, was tested for these substances. As seen in figure 5, the parameter a is plotted with respect to the alloy concentration. A rough linear relation is seen. When fitted with a linear relation we obtain a reduced chi-sqaured value of 3.99 ± 0.02. This indicates the non-linear terms of the relation are indeed contributing.

3.3 Crystal Structure of Copper Gold Alloys

We investigated two samples of copper gold alloy. From the raw data (seen in Appendix A and summarised in table 1), it can be seen that one sample presented many more diffraction peaks than the other, indicating different structures. As Copper and gold are known to have ordered and disordered structures respectively, it is likely this is the reasoning for the difference in diffraction pattern [7].

As outlined in the introduction, if the system is in ordered structure, the copper gold alloy will exhibit characteristics of a simple cubic lattice and produce additional diffraction peaks. If the system is in a disordered condition, the copper gold alloy will be face centered cubic. From the raw data, we believe that sample B is the ordered structure and sample A the

	Peak	θ_{avg}	$\sin^2\theta_{avg}$	$\dfrac{\sin^2\theta_{avg}}{\sin^2\theta_{avg\_min}}$	$3 \cdot \dfrac{\sin^2\theta_{avg}}{\sin^2\theta_{avg\_min}}$	$h^2 + k^2 + l^2$	**a (nm)**
Errors	N/A	0.01	0.002	0.003	0.006	NA	0.02
A	1	0.36	0.127	1.000	3.000	3	0.38
	2	0.42	0.169	1.334	4.003	4	0.38
	3	0.48	0.212	1.667	5.002	5	0.37
	4	0.62	0.339	2.668	8.003	8	0.38
	5	0.75	0.466	3.667	11.01	11	0.38
	6	0.79	0.509	3.998	11.996	12	0.38
B	1	0.21	0.042	1.000	N/A	1	0.34
	2	0.30	0.085	2.009	N/A	2	0.37
	3	0.36	0.127	3.011	N/A	3	0.38
	4	0.42	0.170	4.014	N/A	4	0.38
	5	0.48	0.212	5.017	N/A	5	0.37
	6	0.53	0.255	6.024	N/A	6	0.37
	7	0.62	0.339	8.025	N/A	8	0.38
	8	0.75	0.466	11.03	N/A	11	0.38
	9	0.79	0.587	12.03	N/A	12	0.38

Table 1: Table of average angle and the sum of the Miller indices squared with the approximate lattice constant for given peaks.

disordered. This is confirmed by fitting the individual peaks and finding the corresponding Miller indices. Table 1 illustrates the possible integer value of $h^2 + k^2 + l^2$ according to the average value of the angle θ. Sample B has the set of values of Miller indices that belong to a primitive cubic lattice. On the other hand, sample A features face centered cubic lattice. Thus showing sample B is the ordered state and sample A the disordered.

3.4   Crystal Structure of Lead Tin Alloys

The fitting analysis was also performed on lead tin alloys to determine the peaks of this alloy. Again, the mean values of the double peaks were taken and fit with a linear relation to the corresponding Miller indices. This linear fit is shown in figure 6 and figure 7, respectively. Lattice constant values were determined to be 4.953 ± 0.001 $\mathring{A}$ for pure Pb and 6.462 ± 0.002 $\mathring{A}$ for pure Sn. These values are consistent with the literature values of 4.9052 $\mathring{A}$ for Pb and 6.4892 $\mathring{A}$ for pure Sn [6].
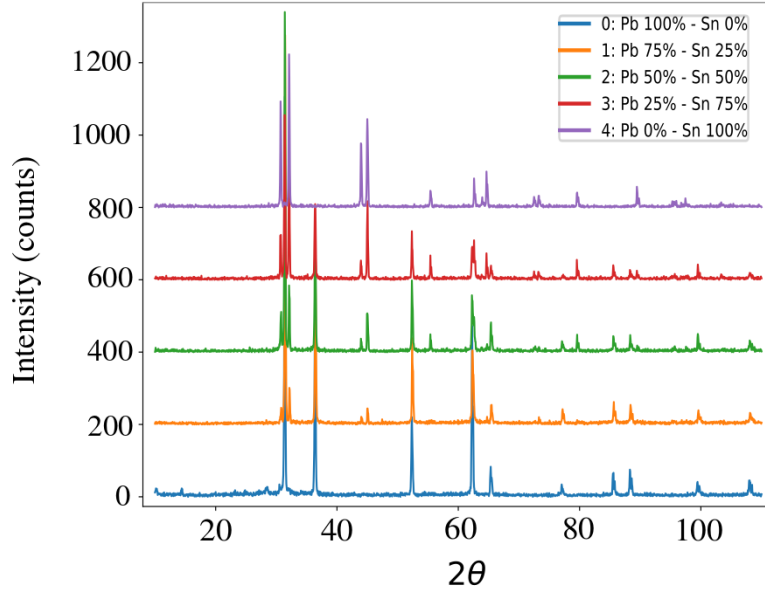
Figure 8: Plot of signal intensity verses angle 2θ of all five PbSn alloy samples with different concentrations. The 50% alloy shows all the peaks of both lead and tin with similar intensity, whereas the 75% lead and 25% tin alloy shows the peaks of lead with larger intensity than the peaks of tin. This indicates that the two substances are not forming a new structure but staying isolates. This may be due to the dramatic difference in lattice constants.
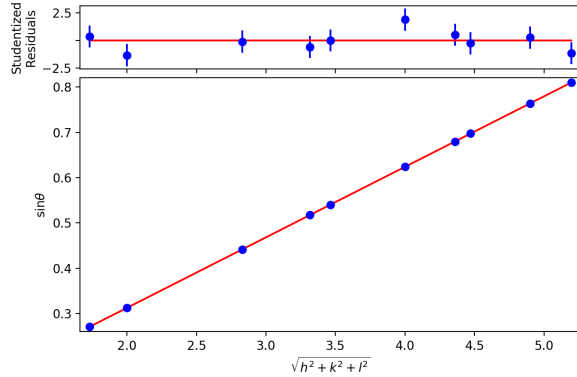
Figure 6: A linear fit of the squared root sum of the 3 Miller indices squared versus $\sin\theta$ of 100% Pb alloy. The slope of this fit was determined to be 0.1557 ± 0.0003 with the y-intercept 0.0001 ± 0.0001. The reduced chi-square value is 0.94 ± 0.51. The lattice constant was determined to be 4.953 ± 0.001 Å
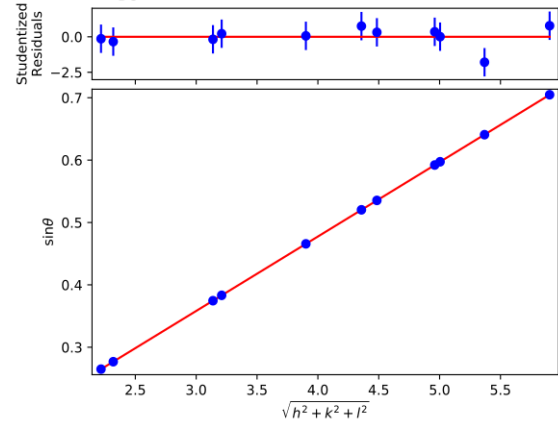
Figure 7: A linear fit of the squared root sum of the 3 Miller indices squared versus $\sin\theta$ of 100% Sn alloy. The slope of this fit was determined to be 0.1193 ± 0.0003 with the y-intercept 0.0002 ± 0.0001. The reduced chi-square value is 0.54 ± 0.47. The lattice constant was determined to be 6.462 ± 0.002 Å.

The diffraction pattern for different concentrations of this alloy seen in figure 8 differs from that of the CuNi alloy. Instead of the peak position varying with concentration, the intensity of the peaks of each substance decreases with the decrease of that substance's concentration.

4 Conclusion

X-ray diffraction allows the crystal structure of a substance to be probed, leading to invaluable insights of the material properties of both pure substances and alloys. Throughout the experiment, diffraction patterns were analyzed to understand the crystal structures of copper nickel, copper gold, and lead tin alloys. Each of these alloys exhibited different structures even though the individual substances all have a cubic unit cell. The copper nickel alloys presented a face centered cubic structure in which the lattice parameter seemed to vary linearly with substance concentration. However, the linear relationship is not truly accurate, suggesting some correction terms to Vegard's law are necessary. The relationship between alloy composition, original structure and mixed structure is not always so simple, as demonstrated with the two Cu_3Au alloys. Difference in manufacturing lead to physical differences in crystal structure of the alloy: an ordered state with simple cubic structure and the other disordered state with a face centered cubic structure. Finally, lead tin alloys were analyzed with the same diffraction method. Here, the differences in each pure substances' structures led to non-cohesive alloys. In all three cases, the method of analysis yielded lattice parameter values in agreement with literature, demonstrating its validity. Looking forwards, x-ray diffractometer analysis could be further extended to wider ranges of alloys: from non-cubic structures to alloys containing more than two metals.

References

[1] S. W. Bracc, "The significance of crystal structure," *Journal of the Society of Chemical Industry*, vol. 41, no. 17, pp. 366–368, 1922. [Online]. Available: https://onlinelibrary.wiley.com/doi/abs/10.1002/jctb.5000411704 1

[2] G. A. Jeffery, "Elements of x-ray diffraction (cullity, b. d.)," *Journal of Chemical Education*, vol. 34, no. 4, p. A178, 1957. 1, 3

[3] C. Kittel, *Introduction to Solid State Physics*, 8th ed. Wiley, 2004. 1, 2

[4] J. B. Calvert, "Crystals and lattices," 2004. 1

[5] V. A. Lubarda, "On the effective lattice parameter of binary alloys," vol. 35, no. 1-2, 2002, p. 53–68. 3, 7

[6] A. Denton and N. W. Ashcroft, "Vegard's law," *Phys. Rev. A*, vol. 43, pp. 3161–3164, 03 1991. 3, 8

[7] C. Suryanarayana and M. Grant Norton, *X-Ray Diffraction: A Practical Approach*, 10 1998, vol. 4. 3, 7
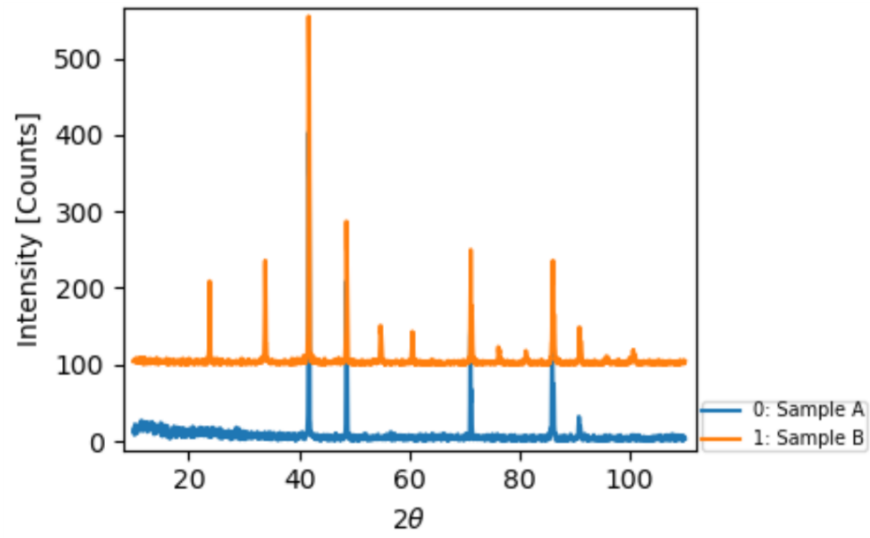
5 Appendix A: Data plots for Pb/Sn and Cu/Au Alloys

Figure 9: Raw peak data of the two types of copper goal alloys.

6 Appendix B: Table of 2θ Values Retrieved with Double Peak Fitting

The tables shown below give experimental values of the two 2θ angles for each of the double peaks, for each alloy.

Sample	Peak	2θ_1	Err 2θ_1	2θ_2	Err 2θ_2	X^2	Err X^2
100% Cu	1	43.40	0.04	43.5	0.1	1.1	0.2
100% Cu	2	50.69	0.05	50.62	0.06	1.2	0.2
100% Cu	3	74.15	0.03	74.35	0.05	1.0	0.2
100% Cu	4	90.02	0.03	90.3	0.1	0.9	0.2
100% Cu	5	95.13	0.02	95.40	0.07	0.8	0.2
75% Cu 25% Ni	1	43.734	0.002	43.36	0.02	1.0	0.2
75% Cu 25% Ni	2	51.16	0.03	51.02	0.02	1.4	0.2
75% Cu 25% Ni	3	74.69	0.03	74.90	0.01	1.0	0.2
75% Cu 25% Ni	4	91.1	0.1	91.36	0.06	0.8	0.2
75% Cu 25% Ni	5	96.10	0.06	96.5	0.1	1.2	0.2
50% Cu 50% Ni	1	43.90	0.03	44.10	0.01	0.8	0.2
50% Cu 50% Ni	2	51.3	0.1	51.36	0.04	1.0	0.2
50% Cu 50% Ni	3	75.19	0.02	75.50	0.01	1.0	0.2
50% Cu 50% Ni	4	91.4	0.2	91.8	0.2	0.8	0.2
50% Cu 50% Ni	5	97.04	0.09	97.07	0.04	0.8	0.2

Sample	Peak	2θ_1	Err 2θ_1	2θ_2	Err 2θ_2	X^2	Err X^2
25% Cu 75% Ni	1	44.4	0.1	44.41	0.10	1.0	0.2
25% Cu 75% Ni	2	51.50	0.08	51.72	0.05	1.2	0.2
25% Cu 75% Ni	3	75.95	0.07	76.2	0.1	1.0	0.2
25% Cu 75% Ni	4	92.31	0.05	92.78	0.05	1.2	0.2
25% Cu 75% Ni	5	97.7	0.2	98.0	0.2	0.9	0.2
100% Ni	1	44.52	0.01	44.592	0.002	1.4	0.3
100% Ni	2	51.935	0.006	52.03	0.05	1.5	0.2
100% Ni	3	76.45	0.03	76.71	0.07	1.1	0.2
100% Ni	4	93.06	0.03	93.46	0.08	1.0	0.2
100% Ni	5	98.48	0.02	98.64	0.02	0.8	0.2

Sample	Peak	2θ_1	Err 2θ_1	2θ_2	Err 2θ_2	X^2	Err X^2
100% Pb	1	31.413	0.009	31.42	0.02	1.4	0.2
100% Pb	2	36.41	0.02	36.34	0.02	1.1	0.2
100% Pb	3	52.32	0.01	52.44	0.04	1.1	0.3
100% Pb	4	62.232	0.004	62.395	0.009	1.0	0.2
100% Pb	5	65.333	0.005	65.508	0.009	0.9	0.2
100% Pb	6	77.10	0.01	77.34	0.01	1.1	0.1
100% Pb	7	85.516	0.004	85.78	0.01	0.9	0.2
100% Pb	8	88.293	0.009	88.56	0.02	0.8	0.2
100% Pb	9	99.438	0.007	99.78	0.01	0.8	0.2
100% Pb	10	107.990	0.007	108.40	0.01	0.8	0.1

Sample	Peak	2θ_1	Err 2θ_1	2θ_2	Err 2θ_2	X^2	Err X^2
75% Pb 25% Sn	1	31.4755	0.003	31.483	0.009	3.1	0.4
75% Pb 25% Sn	2	32.1627	0.007	32.25	0.03	2.1	0.4
75% Pb 25% Sn	3	36.406	0.008	36.456	0.003	0.9	0.2
75% Pb 25% Sn	4	44.01	0.05	44.07	0.02	1.1	0.2
75% Pb 25% Sn	5	44.969	0.009	45.07	0.02	1.1	0.3
75% Pb 25% Sn	6	52.396	0.005	52.531	0.008	0.7	0.2
75% Pb 25% Sn	7	62.283	0.005	62.43	0.04	1.1	0.2
75% Pb 25% Sn	8	64.666	0.007	64.85	0.01	1.2	0.2
75% Pb 25% Sn	9	65.393	0.007	65.56	0.02	0.8	0.2
75% Pb 25% Sn	10	77.21	0.01	77.43	0.01	0.7	0.2
75% Pb 25% Sn	11	85.64	0.08	85.89	0.01	0.8	0.2
75% Pb 25% Sn	12	88.43	0.01	88.72	0.01	0.9	0.2
75% Pb 25% Sn	13	99.59	0.01	99.90	0.03	0.9	0.2
75% Pb 25% Sn	14	108.14	0.02	108.53	0.07	0.7	0.3

Sample	Peak	2θ_1	Err 2θ_1	2θ_2	Err 2θ_2	X^2	Err X^2
50% Pb 50% Sn	1	30.78	0.06	30.85	0.09	1.5	0.4
50% Pb 50% Sn	2	31.307	0.006	31.51	0.02	0.9	0.5
50% Pb 50% Sn	3	32.1	0.1	32.18	0.07	1.7	0.5
50% Pb 50% Sn	4	36.373	0.02	36.46	0.04	1.5	0.2
50% Pb 50% Sn	5	43.941	0.02	44.02	0.02	0.7	0.3
50% Pb 50% Sn	6	44.9699	0.007	45.05	0.01	1.0	0.3
50% Pb 50% Sn	7	52.354	0.007	52.49	0.02	1.0	0.2
50% Pb 50% Sn	8	55.4227	0.003	55.56	0.01	0.7	0.3
50% Pb 50% Sn	9	62.2812	0.006	62.44	0.03	1.1	0.2
50% Pb 50% Sn	10	64.6562	0.006	64.85	0.01	0.8	0.2
50% Pb 50% Sn	11	65.393	0.007	65.56	0.01	0.9	0.3
50% Pb 50% Sn	12	72.678	0.05	73.23	0.03	0.8	0.2
50% Pb 50% Sn	13	77.16	0.01	77.42	0.01	0.6	0.2
50% Pb 50% Sn	14	79.6017	0.004	79.84	0.01	0.9	0.0
50% Pb 50% Sn	15	85.5993	0.010	85.85	0.02	0.9	0.2
50% Pb 50% Sn	16	88.3619	0.008	88.63	0.01	1.1	0.2
50% Pb 50% Sn	17	99.5407	0.006	99.87	0.01	1.1	0.2
50% Pb 50% Sn	18	108.531	0.008	108.53	0.02	0.9	0.2

Sample	Peak	2θ_1	Err 2θ_1	2θ_2	Err 2θ_2	X^2	Err X^2
25% Pb 75% Sn	1	30.668	0.005	30.735	0.007	0.8	0.3
25% Pb 75% Sn	2	31.388	0.003	31.48	0.02	1.0	0.3
25% Pb 75% Sn	3	32.056	0.005	32.139	0.006	1.5	0.3
25% Pb 75% Sn	4	36.340	0.008	36.41	0.02	1.3	0.2
25% Pb 75% Sn	5	43.90	0.02	43.99	0.03	1.1	0.2
25% Pb 75% Sn	6	44.967	0.003	45.079	0.006	1.1	0.2
25% Pb 75% Sn	7	52.35	0.01	52.48	0.02	1.1	0.2
25% Pb 75% Sn	8	55.388	0.005	55.50	0.03	1.0	0.2
25% Pb 75% Sn	9	62.267	0.004	62.56	0.01	1.2	0.2
25% Pb 75% Sn	10	65.357	0.004	65.562	0.008	1.4	0.2
25% Pb 75% Sn	11	72.464	0.006	72.69	0.02	1.6	0.2
25% Pb 75% Sn	12	73.246	0.007	73.45	0.02	0.8	0.3
25% Pb 75% Sn	13	79.573	0.003	79.806	0.006	1.3	0.2
25% Pb 75% Sn	14	85.572	0.005	85.820	0.009	1.0	0.2
25% Pb 75% Sn	15	89.519	0.008	89.80	0.01	0.9	0.2
25% Pb 75% Sn	16	99.501	0.005	99.832	0.007	0.9	0.2
25% Pb 75% Sn	17	108.092	0.008	108.48	0.01	0.8	0.2

Sample	Peak	$2\theta\_1$	Err $2\theta\_1$	$2\theta\_2$	Err $2\theta\_2$	X^2	Err X^2
100% Sn	1	30.701	0.009	30.734	0.005	1.2	0.2
100% Sn	2	32.14	0.03	32.134	0.008	1.4	0.3
100% Sn	3	43.92	0.01	44.08	0.03	1.1	0.3
100% Sn	4	45.00	0.01	45.13	0.02	0.8	0.3
100% Sn	6	55.44	0.01	55.60	0.02	0.7	0.2
100% Sn	7	62.620	0.007	62.79	0.01	1.0	0.3
100% Sn	8	64.659	0.005	64.825	0.007	1.2	0.2
100% Sn	9	72.52	0.01	72.7	0.01	0.7	0.5
100% Sn	10	73.26	0.01	73.5	0.03	0.6	0.5
100% Sn	11	79.587	0.008	79.8	0.01	0.7	0.3
100% Sn	12	89.499	0.007	89.8	0.01	1.0	0.2

Sample	Peak	$2\theta\_1$	Err $2\theta\_1$	$2\theta\_2$	Err $2\theta\_2$	X^2	Err X^2
Cu3Au Sample A	1	41.74	0.02	41.84	0.02	1.2	0.3
Cu3Au Sample A	2	48.59	0.01	48.72	0.02	1.0	0.3
Cu3Au Sample A	3	54.77	0.03	54.92	0.04	0.5	0.3
Cu3Au Sample A	4	71.144	0.008	71.36	0.02	1.2	0.3
Cu3Au Sample A	5	86.012	0.006	86.29	0.01	1.5	0.3
Cu3Au Sample A	6	90.842	0.007	91.14	0.01	0.7	0.3
Cu3Au Sample B	1	23.72	0.04	23.75	0.08	1.1	0.3
Cu3Au Sample B	2	33.88	0.01	33.90	0.07	0.9	0.3
Cu3Au Sample B	3	41.754	0.008	41.87	0.01	1.6	0.3
Cu3Au Sample B	4	48.59	0.01	48.72	0.02	1.0	0.3
Cu3Au Sample B	5	54.77	0.03	54.92	0.04	0.5	0.3
Cu3Au Sample B	6	60.56	0.04	60.68	0.06	0.4	0.4
Cu3Au Sample B	7	71.144	0.008	71.36	0.02	1.2	0.3
Cu3Au Sample B	10	86.012	0.006	86.29	0.01	1.5	0.3
Cu3Au Sample B	11	90.842	0.007	91.14	0.01	0.7	0.3

Lab Book: X-Ray Diffraction

Elisa Jacquet, Alev Orfi, An Vuong

09/01:
- Learnt how to use the x-ray diffractometer and set up the programs
- Samples need to be analysed
    - 1 mystery sample
    - 2 Cu3Au alloys
    - CuNi and PbSn alloys

- Diffractometer parameter1 (param1 from now on) file:
    - Scantype: locked coupled
    - Scan mode : step scan
    - step size (for 2 theta): 0.05deg / 2s
    - initial 2 theta angle: 10 deg
    - final 2 theta angle: 110 deg
    - default generator: 40kV and 40mA

- Wavelength of the diffractometer that is incident upon our sample is: lambda = 0.154nm

Data Collection Step #1:
- Obtain the data for CuNi and PbSn alloys using parameter 1 set-up
    - The data we obtain from the x-ray diffractometer is: the number of x-rays incident upon the detector when the detector is at a particular angle relative to the sample.
    - We call the angle of the detector 2 theta.
    - The way in which we set up the equipment, the detector moves in increments of 0.05 degrees and counts the x-rays for 2 seconds at each position.

Data Collection Step #2:
- Collect data for the rest of the samples: 2 Cu3Au samples with parameter1 set-up

Data Collection Step #3:
- If we need to, do another run of data collection on all samples by focusing the diffractometer to collect more data points around the peaks.

Data Analysis Step #1:
- Solve for the lattice structure of the CuNi and PbSn alloys :
    - Calculate "a": the lattice constant
    - The data will show peaks in counts at particular values of 2*theta. From this, we can solve for "a" and for the miller indices.
- Need to get an idea of how the different concentrations of metals within the alloy reflects on the data and miller indices / lattice constants. -> place to start: plot the counts vs angle for each alloy on the same set of axes to compare.
- Starting point: conduct analysis for 100% Cu to get the code running and the fit working. (Work on automating the process for the other trials).

Samples run in the day : (using param1)
- Cu 100%
- Ni 100%
- Cu 75% , Ni 25%
- Cu 50%, Ni 50%

Example of monitoring data as diffractometer is running:
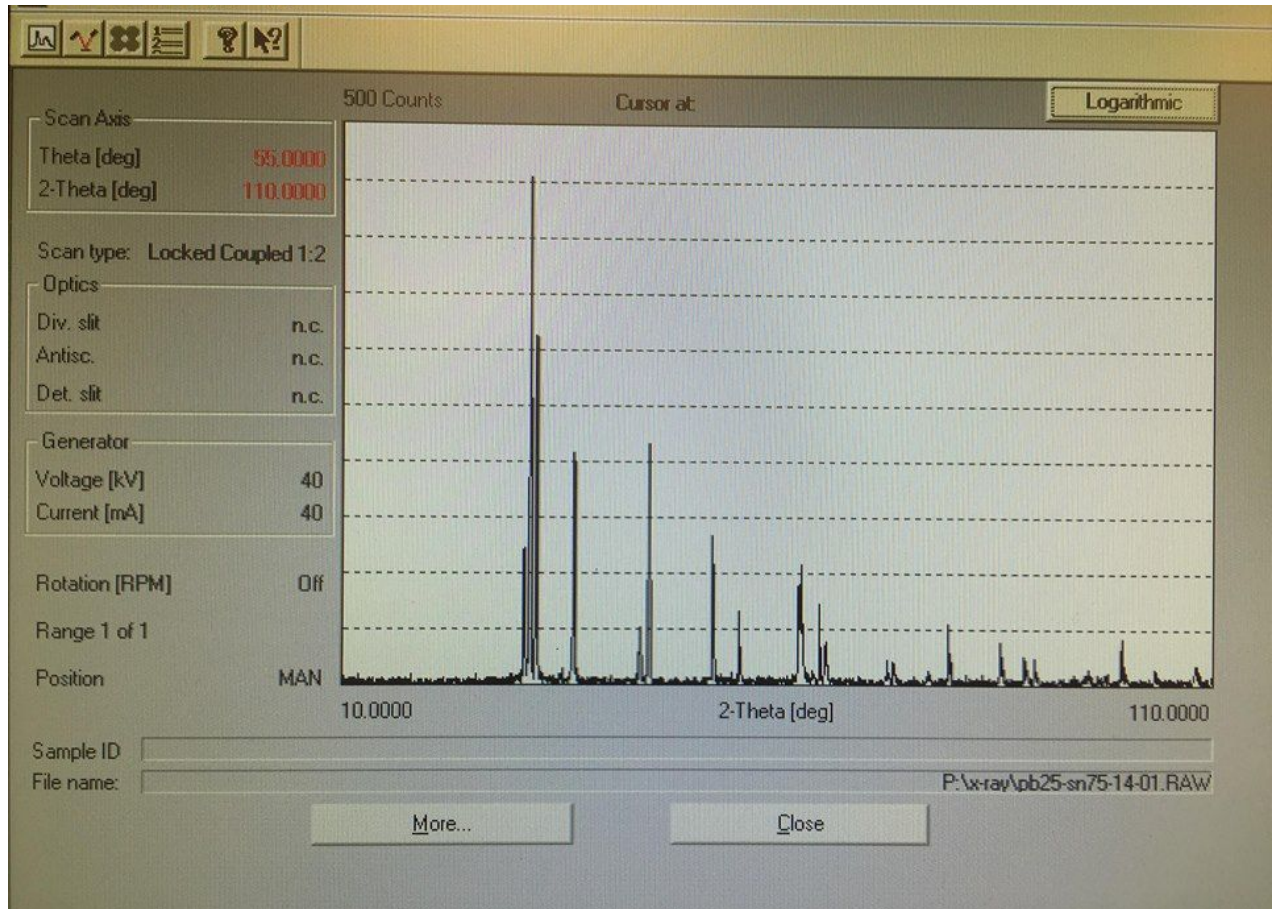
- The angle 2 theta at each peak is what we will need in order to solve for the lattice constant and miller indices.

10/01:
Samples run in the day : (using param1)
- Cu 25%, Ni 75%
- Pb 100%
- Sn 100%
- Pb 75%, Sn 25%

14/01:
Samples run in the day: (using param1)
- Pb 50%, Sn 50%
- Pb 25%, Sn 75%
- Cu3Au sample A
- Cu3Au sample B

Miller Indices and Characterisation of lattices:

Copper is FCC
Nikel is FCC
Lead is FCC
Gold is FCC
Tin is Cubic Diamond structure

For FCC, h, k and l must be either all odd or all even to have peaks
Combinations are: 111, 200, 220, 222

01/23:
Observations:
From looking at the PbSn graphs we can see that the Pb and Sn exist in different sections in the lattice. The 100% Pb showed certain peaks and the 100%Sn showed others and the alloys showed all the peaks. This is different than the CuNi alloys where the peaks only moved position, indicating a change in *a*.

Updated Goals:
1. While graphing the PbSn it's evident we need more data points to obtain good resolution of the double peaks. Goal: go back to the lab and rerun with new parameters
2. Try plotting voigt on double peak (addition of two voigt functions)
3. Get "a" values for all the different alloys - CuNi and PbSn: see how the value of "a" changes for each alloy, an explanation why, and what the structure looks like.
4. Compare our values of "a" with accepted data - especially for pure copper and pure nickel
5. Gold/Copper alloy:
    a. Each sample (A and B) was made with different methods and so they should have a different structure.
    b. Find the structure of each sample and compare them

01/24:
- New data collection for 100% Pb alloy with new parameter file (x-ray diffractometer set up)
    - NOTE: this takes 3hr to run so need to give enough time to run through all PbSn samples !
- Param2 (new set-up for experiment):
    - Scantype: locked coupled
    - Scan mode : step scan
    - step size (for 2 theta): 0.025deg / 3s
    - initial 2 theta angle: 10 deg
    - final 2 theta angle: 110 deg
    - default generator: 40kV and 40mA

- After talking to Robert Gagnon, decided it is better to both decrease the step size in the diffractometer and increase the amount of time for each step. This is the best way to minimize noise and make the peaks really stand out.

01/28:
Peak Fitting Tutorial:
- Reduced Chi^2 values should be as close to 1 as possible.
- The single - peak fits that we did for CuNi alloys are actually not as good as we thought: need to go over the code and write a new fitting function to fit for double peaks
    - This comes from the fact that the beam incident upon the sample in the x-ray diffractometer is not really monochromatic since it contains the two k(alpha) copper wavelengths.
    - We need to treat all the peaks as double peaks.

Vergard's Law:
- Is based on experimental observation that some binary alloy's lattice parameters will change linearly with change in concentration.
- According to these two papers, Vergard's law does not always hold. It only holds if the two metals making up the alloy share certain property (mainly have atomic radii of similar size):
    - http://newmaeweb.ucsd.edu/~vlubarda/research/pdfpapers/mm-03.pdf?fbclid =IwAR1kvXv3dDt8MGNie6gs_OtETsXvh3l87nhg5oGd5fEDK6DTBaNrem4-E qY
    - https://www.researchgate.net/publication/235550709_Vegard's_law
- Verify this with our data, since we already found in interim report that the relationship between concentration and lattice parameter of CuNi alloys changes linearly with change in concentration .
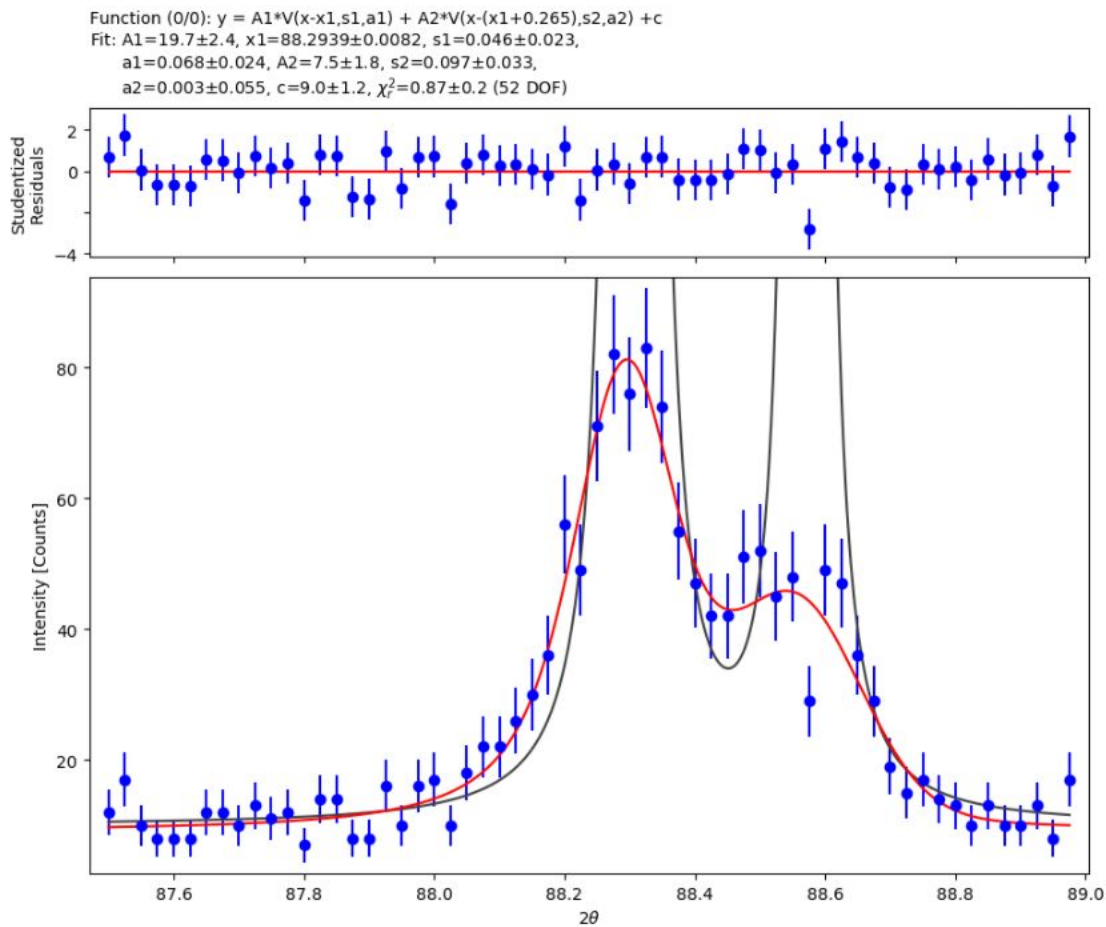
Additional Crystal Structure Research on PbSn:
PbSn:
https://link.springer.com/chapter/10.1007%2F10542753_2419

01/30:

- Got the double peak fitting to work with much better reduced chi-squared. See below sample graph:

Function (0/0): $y = A1*V(x-x1,s1,a1) + A2*V(x-(x1+0.265),s2,a2) +c$
Fit: A1=19.7±2.4, x1=88.2939±0.0082, s1=0.046±0.023,
a1=0.068±0.024, A2=7.5±1.8, s2=0.097±0.033,
a2=0.003±0.055, c=9.0±1.2, χ_r^2=0.87±0.2 (52 DOF)

- **Ran sample**: 75%Pb 25%Sn with param2 file
- Performed the double fit for all the peaks in the CuNi series of data (i.e for each alloy, all the peaks were fitted and tabulated)

01/31:

- **Ran samples**: 50%Pb 50%Sn and 25%Pb 75%Sn with param2 file
- Work on analysis and report writing
- Perform double peak fit for Cu3Au data samples

02/01:

- **Ran sample**: 100%Sn with param2 file (completes data collection)
- Perform double peak fit for all PbSn data
- Keep working on writing report